https://doi.org/10.48048/tis.2022.4912

Molecular Structure, Vibrational Studies and Reactivity Descriptors Analysis of 4-[2-(tert-butylamino)-1-hydroxyethyl]-2-(hydroxymethyl)Phenol

Rubarani P. Gangadharan

Department of Physics, Rajalakshmi Engineering College, Tamil Nadu 602105, India

(Corresponding author's e-mail: rubarani.p.gangadharan@rajalakshmi.edu.in)

Received: 27 June 2022, Revised: 2 August 2022, Accepted: 9 August 2022, Published: 1 November 2022

Abstract

The compound 4-[2-(tert-butylamino)-1-hydroxyethyl]-2-hydroxymethyl)phenol (4BAHEHMP)was chosen for investigation and characterized by FT- IR and FT- Raman spectral analysis. The compound has been studied significantly by using density functional theory (DFT) calculations by the B3LYP method at the 6-31++G(d,p) basis set level. The calculated results show that the structural parameters can be reproduced well with the predicted geometry. The experimental vibrational frequencies were compared with the scaled vibrational frequencies for the assignment of vibrational bands. In addition to the DFT calculations of the compound, the calculations were performed for Fukui functions to explain the chemical selectivity or reactivity sites such as the molecule's nucleophilic, electrophilic, and radical attack in the compound. Mulliken atomic charges are calculated for the determination of electronic charge distribution and reactive sites which proves the formation of intermolecular interaction in solid forms provided by the significant region of electronegativity around oxygen atoms and the net positive on hydrogen and nitrogen atoms.The chemical and thermal stability of the compound is studied by using DFT method for different temperatures and it shows that thermodynamic parameters increase with increase in temperature.

Keywords: DFT, MPA, Fukui functions, Enthalpy

Introduction

4-[2-(tert-butylamino)-1-hydroxyethyl]-2-(hydroxymethyl)phenol is a short-acting agonist of the β2-adrenergic receptor. It is called by the name salbutamol. It is a β2-mimetic that is utilized in medications such as controlled-release pills, syrups, inhalers, nebulizers, and injections as a bronchodilator. Its chemical formula is $C_{13}H_{21}NO_3$. It is used to treat COPD, also known as chronic obstructive pulmonary disease, and asthma. This substance was chosen because it resembles adrenaline, the body's own naturally occurring bronchodilator. The bronchioles that supply air deep into the lungs become inflamed as a result of asthma or COPD attacks. The muscles in the walls of the lungs constrict, causing the lungs to become narrow, which is extremely hazardous and potentially fatal. During this time, the particular shape of adrenaline will enable the molecule fit into the active areas on the muscular wall cells. The airways widen as a result of the muscles relaxing. This action is known as bronchodilation. It was identified based on how adrenaline affects the bronchioles and is also known as albuterol [1]. The typical method of therapy uses a metered dosage inhaler, nebulizer, or other specialized delivery systems like Rotahaler or Autohaler to have a direct impact on the bronchial smooth muscle. The inhaler ensures that very small amounts of medication are delivered directly into the lungs. This drug has been used to treat acute hyperkalemia, as it stimulates potassium flow into cells, thus lowering the potassium in the blood.

This compound 4-[2-(tert-butylamino)-1-hydroxyethyl] which we will investigate, is also known as 4BAHEHMP. The primary aim of this research is to determine the theoretical approaches utilized to calculate the vibrational wave numbers and molecular structural characteristics. By employing the basis set of 6-31++G(d,p) and the Gaussian 03W software, the DFT/B3LYP technique generates the structure optimization and other input files. Investigating reactions processes is made feasible by computation predictions based on DFT [2]. In the current research, DFT was used to investigate a number of different aspects of molecular structure, including its vibrational frequencies, varied bond lengths and bond angles, Fukui functions, and Mulliken atomic charges.

Experimental section

The sample of 4-[2-(tert-butylamino)-1-hydroxyethyl]-2-(hydroxymethyl)phenolfor study in the solid form was purchased from the sigma Aldrich with a purity of greater than 99% and it is used as such without further purification. It is in powder form at room temperature. The FTIR spectrum of molecule was recorded in the region 4,000 - 450 cm^{-1} on a BRUKER IFS 66V spectrometer and calibrated using polystyrene bands. The sample was prepared by using KBr disc. The FT-Raman spectrum of the sample was recorded between 4,000and 100 cm^{-1} regions on a Bruker FRA 106/S FT-Raman instrument using 1,064 nm excitation from an Nd:YAG laser and the spectral data have been collected at Sophisticated Analytical Instruments Facility Indian Institute of Technology (Madras) at Chennai, India. The detector is a liquid nitrogen cooled Ge detector.

Computational details

The computational details for geometry optimization and electronic structure of the compound have been carried out by density functional theory [3] by using the Gaussian 03W program package [4] using the different basis sets and Becke's3 parameter hybrid exchange functional with Lee-Yang-Parr correlation functional (B3LYP) [5-7]. By usingGauss view program [8] with symmetry considerations, vibrational frequency assignments were calculated with a high accurate value. Infrared absorption intensities and Raman intensities have been computed in the harmonic approximation by using the same functional and basis sets used for the optimized geometries, from the derivatives of the dipole moment and polarizability of each normal mode, respectively. The vibrational wavenumbers which have been calculated are considered as scaled values. The electronic charge distribution in a molecule was calculated by using Mulliken population analysis.

Results and discussion

Geometry optimization

The theoretical structure of title molecule have been calculated by DFT methodby using the Gaussian 03W software package and geometry obtained from B3LYP/6-31++G(d,p) is displayed in **Figure 1**. By comparing the structure it can be justified that the bond lengths determined from this method is slightly different than that obtained from other methods but it yields bond angles in good agreement with each other and also with the experimental values for isolated molecule in gaseous phase and the experimental results are for a molecule in a solid state [9].

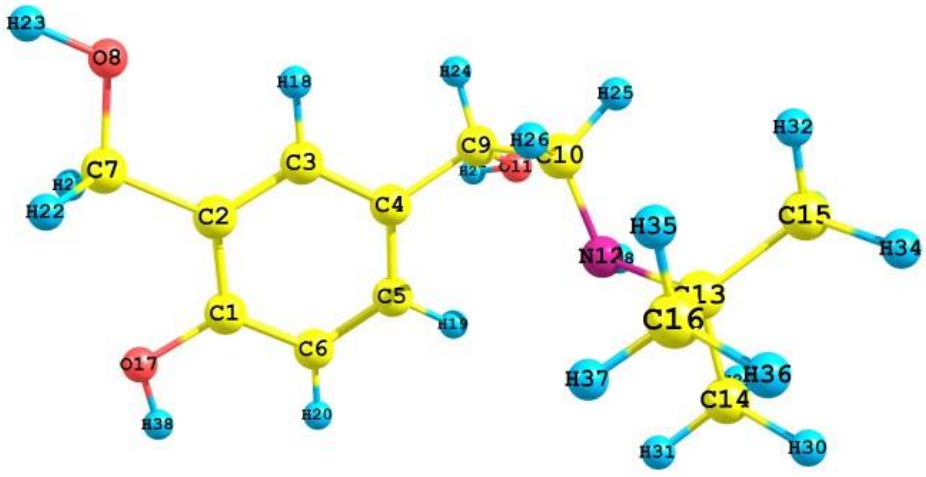

Figure 1 Optimized molecular structure and atomic numbering of 4BAHEHMP.

The optimized geometrical parameters such as bond lengths and bond angles for this compound are calculated by DFT/B3LYP levels with the 6-31++G(d,p) basis set and are listed in **Table 1**. The calculated geometrical parameters obtained at the DFT level of theory are compared with the experimental structural parameters. In **Table 1** the comparison is made between the calculated bond lengths and angles with the

experimentally available data [10]. It can be observed that experimental data agree reasonably well with the calculated parameters.

Table 1 Optimized geometric parameters of 4BAHEHMP by B3LYP/6-31++G(d,p) method.

Parameter	B3LYP/6-31++G(d,p)	experimental	Parameter	B3LYP/6-31++G(d,p)	experimental[a]
Bond length (A°)			**Bond angle(A°)**		
C1-C2	1.402	1.400	C2-C1-C6	120.59	121
C1-C6	1.395	1.375	C2-C1-O17	116.74	118
C1-O17	1.373	1.225	C6-C1-O17	122.65	121.9
C2-C3	1.394	1.385	C1-C2-C3	118.33	117.9
C2-C7	1.509	1.523	C1-C2-C7	119.16	117.73
C3-C4	1.401	1.443	C3-C2-C7	122.5	126.7
C3-H18	1.085	1.096	C2-C3-C4	121.97	121.03
C4-C5	1.399	1.418	C2-C3-H18	117.85	117.8
C4-C9	1.517	1.547	C4-C3-H18	120.16	121.5
C5-C6	1.393	1.416	C3-C4-C5	118.56	118.6
C5-C6	1.083	1.096	C3-C4-C9	119.85	119.5
C5-H19	1.088	1.091	C5-C4-C9	121.57	121.8
C6-H20	1.421	1.372	C4-C5-C6	120.4	121.2
C7-O8	1.102	1.093	C4-C5-H19	119.48	121
C7-H21	1.102	1.097	C6-C5-H19	120.09	120.6
C7-H22	0.964	0.901	C1-C6-C5	120.11	120.99
O8-H23	1.538	1.501	C1-C6-H20	119.65	120.1
C9-C10	1.434	1.415	C5-C6-H20	120.22	121.3
C9-O11	1.102	1.098	C2-C7-O8	109.57	109
C9-H24	1.456	1.382	C2-C7-H21	109.15	107.7
C10-N12	1.104	1.099	C2-C7-H22	109.05	107
C10-H25	1.094	1.082	O8-C7-H21	111.38	111.7
C10-H26	0.966	0.901	O8-C7-H22	111.38	111.7
O11-H27	1.477	1.465	H21-C7-H22	106.18	106.2
N12-C13	1.017	1.014	C7-O8-H23	107.63	109
N12-H28	1.538	1.547	C4-C9-C10	114.7	114.4
C13-C14	1.545	1.547	C4-C9-O11	112.37	112.8
C13-C15	1.539	1.54	C4-C9-H24	107.66	108.6
C13-C16	1.096	1.087	C10-C9-O11	105.58	109
C14-H29	1.094	1.085	C10-C9-H24	106.57	108.35
C14-H30	1.093	1.092	O11-C9-H24	109.74	108.6
C14-H31	1.093	1.092	C9-C10-N12	110.82	110.1
C15-H32	1.094	1.099	C9-C10-H25	107.13	109.9

Parameter	B3LYP/6-31++G(d,p)	experimental	Parameter	B3LYP/6-31++G(d,p)	experimental[a]
Bond length (A°)			**Bond angle(A°)**		
C15-H33	1.096	1.099	C9-C10-H26	107.8	109
C15-H34	1.095	1.099	N12-C10-H25	113.76	112.6
C16-H35	1.094	1.084	N12-C10-H26	109.9	109
C16-H36	1.094	1.084	H25-C10-H26	107.15	107.8
C16-H37	1.093	1.084	C9-O11-H27	107.3	109
O17-H38	0.966	0.900	C10-N12-C13	118.23	115.1
			C10-N12-H28	107.28	107
			C13-N12-H28	109.23	108.5
			N12-C13-C14	106.02	107.3
			N12-C13-C15	113.24	113
			N12-C13-C16	109.26	109
			C14-C13-C15	109.23	109
			C14-C13-C16	109.04	106.3
			C15-C13-C16	109.88	109
			C13-C14-H29	110.88	110
			C13-C14-H30	111.02	111.5
			C13-C14-H31	110.35	111.7
			H29-C14-H30	107.65	109.1
			H29-C14-H31	108.07	109
			H29-C14-H31	108.73	109.1
			C13-C15-H32	111.67	110.5
			C13-C15-H33	110.79	109.97
			C13-C15-H34	111.02	109.79
			H32-C15-H33	107.9	106.1
			H32-C15-H34	107.46	109.2
			H33-C15-H34	107.8	109
			C13-C16-H35	112	111.47
			C13-C16-H36	110.41	111.45
			C13-C16-H37	110.2	111.27
			H35-C16-H36	107.27	108.9
			H35-C16-H37	108.16	109.1
			H36-C16-H37	108.66	109.2
			C1-O17-H38	108.95	109

[a]Taken from [10]

However, due to the solid-state intermolecular interactions associated with crystal packing effects, there are some discrepancies between the predicted values (in the gas phase) and the measured results. Despite these discrepancies, the estimated geometrical parameters are a reliable approximation and serve as the starting point for the computation of other parameters, including vibrational assignments and thermodynamical properties, which are discussed in the next sections.

Vibrational spectral analysis

The vibrational spectral assignments of 4BAHEHMP have been executed with the help of PED analysis.From the theoretical calculations, the molecule has a structure of C_1 point group symmetry. The molecule has 38 atoms and 108 modes of fundamental vibrations. The internal coordinates givesthe information about the position of the atoms in terms of distances and angles with respect to an origin atom which are displayed in **Table 2**. In **Table 3** the fundamental vibrational modes werecalculated using the DFT/B3LYPlevels with 6-31++G (d,p) basis set using Gaussian 03W package. **Table 3** also presents observed FT-IR, FT Raman and scaled wavenumbers with relative intensities. The vibrational bands assignments of the compound have been made by using Gauss-view molecular visualization program. All the vibrations are active both in IR and Raman. The observed and simulated FT-IR and FT-Raman spectra are shown in **Figures 2** and **3**. It is observed that the calculated wavenumbers correspond to the isolated molecular state whereas the observed wave numbers correspond to the solid state spectra. The calculated vibrational wave numbers using B3LYP basis set were compared with experimentally observed values. Some bands which were predicted in the IR and Raman spectra were not observed in the experimental spectrum of 4BAHEHMP. Theoretical harmonic frequencies typically overestimate observed fundamentals due to the neglect of mechanical anharmonicity, electron correlation and basis set effects. Therefore, the scaling factor values of 0.962 for B3LYP method[11,12] is used.

Table 2 Interpretation of internal coordinates of 4BAHEHMP.

No.	Symbol	Type	Definition
		Stretching	
1-6	νi	C-C(Chain)	C2-C7,C4-C9,C9-C10,C13-16, C13-C14,C13-C15
7-12	νi	C-C(Ring)	C1-C2,C2-C3,C3-C4,C4-C5, C5-C6,C6-C1
13-15	νi	C-H(Ring)	C3-H18,C5-H19,C6-H20
16-24	νi	C-H(methyl)	C16-H35,C16-H37,C16-H36,C14-H29, C14-H30,C14-H31,C15-H32,C15-H33,C15-H34
25-28	νi	C-H(CH_2)	C7-H21,C7-22,C10-H26,C10-H25
29-30	νi	C-N	O11-H27,O8-H23,O17-H38
31-33	νi	O-H	O11-H27,O8-H23,,O17-H38
34-36	νi	C-O	C7-O8,C9-O11,C1-O7
37	νi	N-H	N12-H28
38	νi	C-H(CH2)	C9-H24
		Bending	
39-44	βi	C-C-C(Ring)	C1-C2-C3,C2-C3-C4,C3-C4-C5, C4-C5-C6,C5-C6-C1,C6-C1-C2
45-50	βi	C-C-H(Ring)	C2-C3-H18,C4-C3-H18,C1-C6-H20, C6-C5-H19,C4-C5-H19
51-53	βi	C-O-H	C7-O8-H23,C1-O17-H38,C9-O11-H27

No.	Symbol	Type	Definition
54-55	βi	H-C-H	H21-C7-H22,H26,C10,H25
56-64	βi	H-C-H(methyl)	H32-C15-H34,H33-C15-H34,H33-C15-H32, H31-C14-H29,H30-C14-H29,H30-C14-H30, H35-C16-H36,H36-C16-H36,H36-C16-H37
65	βi	C-N-C	C10-N12-C13
66-79	βi	C-C-H(Chain)	C13-C15-H32,C13-C15-H33,C13-C15-H34, C13-C14-H29,C13-C14-H30,C13-C14-H31, C13-C16-H35,C13-C16-H36,C13-C16-H37, C9-C10-H26,C9-C10-H25,C9-C10-H24, C2-C7-H21,C2-C7-H22,C4-C9-H24
80-87	βi	C-C-C(linear)	C16-C13-C15,C14-C13-C16,C14-C13-C15, C3-C2-C7,C1-C2-C7,C3-C4-C9, C5-C4-C9,C4-C9-C10
88-92	βi	O-C-C	O8-C7-C2,O11-C9-C4,O17-C1-C2, O17,C1-C6,O11-C9-C10
93-94	βi	C-N-H	C10-N12-H28,C13-N12-H28
95-98	βi	C-C-N	C9-C10-N1,C14-C13-N12,C15-C13-N12, C16-C13-N12
99-101	βi	O-C-H	O8-C7-H22,O11-C9-H24,O8-C7-H21
102-103	βi	N-C-N	N12-C10-H26,N12-C10-H25
Out of Plane bending			
104-106	ωi	C-H(Ring)	H18-C3-C2-C4,H19-C5-C6-C4,H20-C6-C1-C5
107-112	ωi	C-C(Chain)	C7-C2-C3-C4,C2-C3-C4-C9,C7-C2-C1-C6, C3-C4-C9-C10,C6-C5-C4-C9,C5-C4-C9-C10
113-115	ωi	C-H(methyl)	C14-H31-H29-H30,C16-H36-H35-H37, C15-H32-H33-H34
116	ωi	C-N	N12-C10-C13-H28
117-118	ωi	Butterfly	C7-C2-C1-C6,C3-C2-C1-O17
Torsion			
119-124	τi	C-C(Ring)	C1-C2-C3-C4,C2-C3-C4-C5,C3-C4-C5-C6, C4-C5-C6-C1,C5-C6-C1-C2,C6-C1-C2-C3
125-141	τi	C-H(Linear)	C14-C13-C15-H32,C14-C13-C15-H34,C14-C13-C15-H33, C14-C13-C16-H36,C14-C13-C16-H35,C14-C13-C16-H37, C16-C13-C14-H29,C16-C13-C14-H30,C16-C13-C14-H31, C16-C13-C15-H32,C16-C13-C15-H33,C16-C3-C15-H34, C4-C9-C10-H26,C4-C9-C10-H25,C5-C4-C9-H24 C1-C2-C7-H21,C1-C2-C7-H22

The 3,800-2,200 cm^{-1} region

The vibrational OH and NH stretching modes in the range 3,500 - 3,100 cm^{-1} are not clearly observed in the infrared spectrum as well as in the Raman spectrum, whereas the low wavenumber region bands that are normally characteristic of crystalline pharmaceutical forms are not recorded in the infrared spectrum. The observed infrared and Raman wavenumbers are shown in **Table 3** along with the calculated values. The major experimental vibrational assignments wasaccomplished in the light of the theoretical results and from the vibrational spectroscopic data previously reported [13]. As shown in the **Figure 2** the broad υ OH stretching band in the IR spectrum at 3,525 cm^{-1} frequencydemonstrates the hydrogen bonding in the compound. The CH stretching region consists of several features in the wavenumber range 3,130 - 2,800 cm^{-1} for both infrared and Raman spectra and the CH stretching bands for the aromatic ring of the compound are displayed in the Raman spectra in **Table 3** and can be assigned to the bands at 3,162 and 3,025 cm^{-1}. The CH aliphatic stretching bands of CH_3 symmetric and asymmetric stretching modes are displayed in the both Raman and infrared spectra, and is assigned to the moderate strong features at 2,982, 2,977 and 2,918 cm^{-1} in the infrared spectrum and 2,978, 2,932 and 2,916 cm^{-1} in the Raman spectrum. The broad medium band 2,916 cm^{-1} and the medium band at 2,887 cm^{-1} in the Raman spectrum can be featured to υ CH and υ CH_2 attached to aliphatic OH bands, respectively.

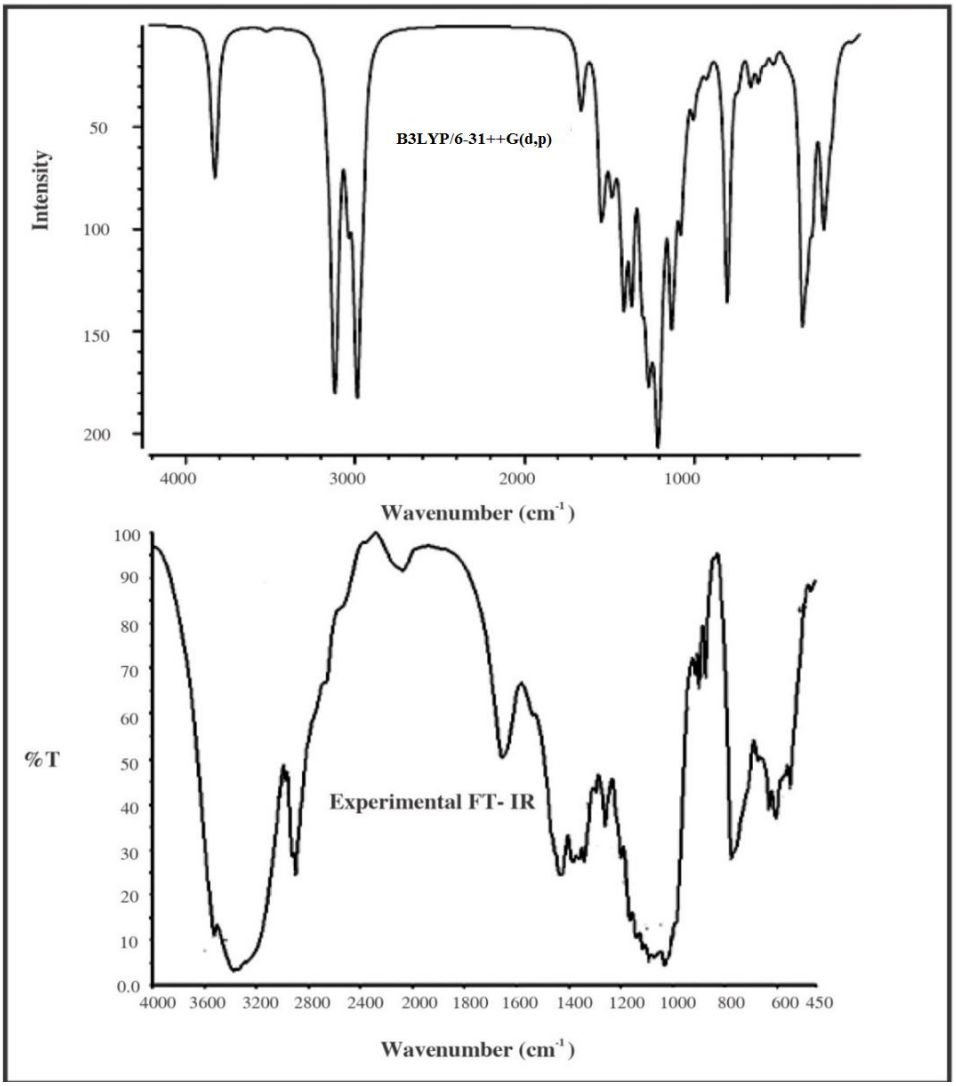

Figure 2 FT-IR spectra of 4BAHEHMP (Theoretical and Experimental).

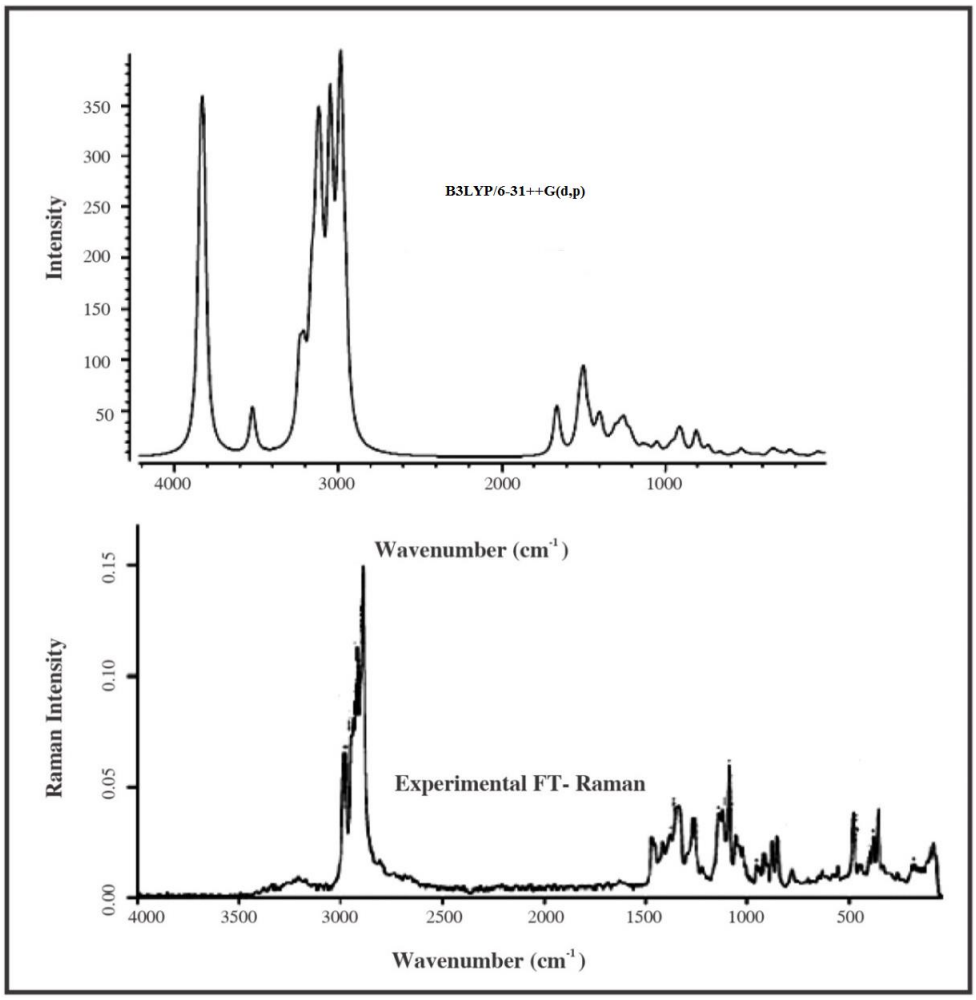

Figure 3 FT-Raman spectra of 4BAHEHMP (Theoretical and Experimental).

Table 3 Observed and calculated vibrational frequencies of 4BAHEHMP.

Mode No.	Observed frequencies (cm^{-1})		Calculated frequencies(cm^{-1})				
	FT-IR	FT-Raman	B3LYP/6-31++G(d,p)		IR intensity[a]	Raman intensity[b]	Vibrational assignments
			Unscaled	Scaled			
1	-	-	3,841	3,695	22.67	99.21	ν OH
2	-	-	3,824	3,678	44.44	65.45	ν OH
3	3,525m	-	3,817	3,671	13.83	51.74	ν OH
4	3,380w	-	3,520	3,386	1.96	22.61	ν NH
5	3,162 s	3,107w	3,233	3,110	3.26	35.87	ν CH_{ring}
6	-	3,093w	3,207	3,085	1.76	28.15	ν CH_{ring}
7	3,025 s	-	3,160	3,039	21.4	50.06	ν CH_{ring}
8	-	-	3,131	3,012	50.37	49.33	$\nu_{as}CH_3$
9	-	-	3,125	3,006	11	11.26	$\nu_{as}CH_3$

Mode No.	Observed frequencies (cm^{-1})		Calculated frequencies(cm^{-1})				
	FT-IR	**FT-Raman**	**B3LYP/6-31++G(d,p)**		**IR intensity[a]**	**Raman intensity[b]**	**Vibrational assignments**
			Unscaled	Scaled			
10	-	-	3,117	2,998	59.57	40.03	$\nu_{as}CH_3$
11	-	-	3,112	2,993	7.52	13.84	$\nu_{as}CH_3$
12	-	2,985m	3,107	2,988	48.87	46.37	$\nu_{as}CH_3$
13	2,982m	-	3,100	2,982	3.05	6.87	$\nu_{as}CH_3$
14	2,977w	2,978vs	3,089	2,971	18.42	17.78	$\nu_{as}CH_2$
15	-	2,932s	3,048	2,932	8.34	100	ν_sCH_3
16	-	2,916s	3,037	2,921	31.4	49.22	ν_sCH_3
17	2,918s	-	3,033	2,917	21.2	3.39	ν_sCH_3
18	2,900s	2,887vs	2,997	2,883	48.06	4.73	ν CH, $\nu_{as}CH_2$
19	-	-	2,983	2,869	74.09	49.49	$\nu_{as}CH_2$
20	-	-	2,977	2,863	43.86	90.24	ν_sCH_2
21	2,793s	-	2,951	2,838	49.9	45.63	ν_sCH_2
22	1,616s	1,656vs	1,668	1,604	28.99	15.41	ν CC_{ring}
23	-	-	1,655	1,592	7.49	11.18	β CC_{ring}, β C-O-H
24	1,558w	-	1,551	1,492	58.33	1.36	β C-O-H
25	-	-	1,535	1,476	9.46	1.32	ν CC_{ring}
26	-	-	1,530	1,471	17.5	3.17	δ CH_2
27	-	1,467m	1,523	1,465	3.69	7.25	$\nu s(CH_2)$
28	-	-	1,517	1,459	4.38	5.81	$\nu s(CH_3)$
29	-	-	1,515	1,457	5.1	4.57	δ CH_3
30	-	-	1,502	1,444	0.28	8.98	δ CH_3
31	-	-	1,498	1,441	11.84	0.36	δ CH_2-N
32	-	-	1,495	1,438	6.12	13.84	δ CH_3
33	-	-	1,488	1,431	12.29	1.56	δ CH_3
34	1,428s	-	1,480	1,423	26.27	2.36	Ring stretch
35	1,409m	1,412m	1,461	1,405	15.52	8.75	Hydrogen bonded C-OH angle δ C-OH
36	1,383s	1,378w	1,436	1,381	14.97	0.85	δCH_2
37	1,362w		1,416	1,362	48.85	2.48	β NH, δ CH_2, δ C-OH
38			1,410	1,356	36.11	2.74	δ OH), δ CH_2
39			1,406	1,352	4.93	5.05	δ CH_3
40	1,342s		1,394	1,341	12.05	8.91	β CH_{ring}
41		1,335m	1,388	1,335	4.08	1.25	ν_s CH_2
42			1,365	1,313	87.31	1.83	β OH, ring vibration
43	1,297m		1,334	1,283	4.64	3.4	ν OH, β CH
44	1,260s	1,261s	1,306	1,256	70.16	6.65	δ CH

Mode No.	Observed frequencies (cm^{-1})		Calculated frequencies(cm^{-1})				
	FT-IR	**FT-Raman**	**B3LYP/6-31++G(d,p)**		**IR intensity[a]**	**Raman intensity[b]**	**Vibrational assignments**
			Unscaled	Scaled			
45	1,244m		1,301	1,251	4.62	2.02	ν CN, δ CH_2
46		1,220w	1,276	1,227	49.39	7.6	β CH
47			1,264	1,215	60.94	0.97	β C-OH angle coupled to phenyl ring vibration
48	1,201s		1,254	1,206	0.64	6.29	Hydrogen bonded C-OH angle coupled to phenyl ring vibration
49			1,248	1,200	0.34	4.43	β CH2, β OH
50			1,242	1,194	40.82	2	δ CH2, δ COH
51			1,217	1,170	74.76	5.45	δ CH3
52	1,167s		1,213	1,166	26.45	1.8	δ C-OH, phenyl ring vibration
53	1,142w		1,198	1,152	74.04	2.21	δ CHOH, ν CN
54		1,138m	1,174	1,129	29.65	1.51	ν CN
55	1115w	1,119m	1,139	1,095	13.67	2.48	Hydrogen bonded C-OH angle coupled to phenyl ring vibration
56	1,072w	1,085vs	1,130	1,087	82.27	0.9	ω CH2
57		1,052m	1,109	1,066	33.03	2.7	νs(CH2)
58	1,034w		1,075	1,034	59.93	1.3	νs CH2OH
59		1,019w	1,051	1,011	3.25	3.09	ρ CH2
60			1,045	1,005	13.33	1.89	ρ(CH3)
61			1,044	1,004	1.19	0.59	νas(COH)
62		951w	1,000	962	24.92	1.05	νas(COH)
63			970	933	2.83	1.14	νas(COH)
64			962	925	6.15	3.19	out of plane δ CH
65	915w	914w	958	921	0.32	0.15	ν CN, β OH
66	899s		930	894	3.59	0.82	δ CH ring
67			927	891	3.74	3.19	δ CH2
68			916	881	3.99	1.7	ν CN
69	876s	875m	911	876	1.86	4.58	δ CC ring
70		850m	899	864	1.56	6.84	νasCN
71			815	784	1.53	1.6	out of plane δ CH ring
72	775vs	777w	810	779	20.6	8.21	νasC-C-O
73			800	769	83.1	1.25	νasC-C-O
74			793	762	25.11	2.07	ω CH, β C-C-C
75		729w	735	707	12.8	4.27	ω CH
76			728	700	1.78	0.26	ω CH

Mode No.	Observed frequencies (cm^{-1})		Calculated frequencies(cm^{-1})				
	FT-IR	**FT-Raman**	**B3LYP/6-31++G(d,p)**		**IR intensity[a]**	**Raman intensity[b]**	**Vibrational assignments**
			Unscaled	Scaled			
77	631s	631w	662	636	19.28	2.02	δ CCC
78	606s		617	593	17.08	0.28	ring deformation
79	551m	553w	576	554	8.36	1.01	out of plane δ CCC ring
80			535	514	6.82	3.14	in plane δ CCN
81			518	498	5.51	0.87	out of plane δ CC
82	471w	475s	486	467	0.26	0.86	δ CC
83		444w	458	440	5.4	0.33	δ CCchain
84			451	433	0.63	0.13	t CC, t CN
85			429	412	2.71	0.36	t CH3, tCC
86		398w	426	409	2.28	0.46	δ CCchain
87		376m	357	343	100	1.37	out of plane CCC
88		356s	352	338	7.29	0.74	out of planeCCC
89			345	331	1.13	0.35	out of planeCCC
90			337	324	6.84	0.25	out of planeCCC
91		312w	327	314	54.36	2.3	in plane(CCC) skeletal deformation
92			296	284	56.33	1.01	in plane(CCC) skeletal deformation
93			283	272	0.23	0.16	ω(CH3)
94			281	270	2.34	0.4	ω(CH3)
95		257w	268	257	0.59	0.1	ω(CH3)
96			238	228	15.34	1.39	ω(CH3)
97			233	224	29.31	1.29	ω(CH3)
98			225	216	29.78	0.66	ω(CH3)
99		193w	205	197	26.14	0.41	ω(CH3)
100		173w	179	173	25.79	0.53	τ(CH3)
101		150w	150	144	0.39	0.14	τ(CH3)
102			141	135	0.96	0.22	skeletal mode
103			137	131	1.31	0.09	skeletal mode
104		83m	94	90	1.04	0.59	skeletal mode
105			63	60	2.75	2.31	skeletal mode
106			43	41	1.82	0.47	skeletal mode
107			21	20	0.23	0.48	δ(CH3)
108			18	17	0.25	1.16	ring breathing

Abbreviations; s-strong; vs-very strong; w-weak; vw-very weak; ν_s- symmetric stretching;
ν_{as}-asymmetric stretching; β-bending, ω- wagging; τ-Torsion; ρ-rocking; δ – scissoring, Butt– butterfly.
[a] Relative absorption intensities normalized with highest peak absorption equal to 100,
[b] Relative activities normalized to 100

The 1,800 - 1,100 cm^{-1} region

This spectroscopic region plays a crucial role for structural studies particularly for the C-C group in this molecule. Expanded wavenumber regions of the infrared and Raman spectra are displayed in **Figure 2**. The infrared region contains a rich spectrum from the C-C functionality and several bands of medium and strong intensities while Raman spectrum consists mainly of the strong C-C characteristics and several other weaker characteristics. The υ C-C band occurs at 1,616 cm^{-1} in infrared and at 1,656 cm^{-1} in the Raman spectrum. The bands at 1,558, 1,409, 1,201, 1,167 and 1,115 cm^{-1} in infrared spectra which are weak bands and not observed in Raman spectrum can be assigned as hydrogen-bonded C–OH angle coupled to phenyl ring vibration based on the theory of quantum chemical calculations. Again, it can be noted that the calculated methyl deformation vibrational bands at 1,457, 1,444, 1,438 and 1,431cm^{-1} have not been observed in the experimental spectra. The calculated scaled values by B3LYP/6-31++G(d,p) at 1,476 and 1,471 cm^{-1} can be assigned to υ CC ring and δ CH_2 modes, respectively. Within the range 1,470 - 1,250 cm^{-1} the CH_3, CH_2 and CH aliphatic bending vibrations bands will occur.

The 1,100 - 50 cm^{-1} region

Infrared and Raman spectra for this wavenumber range are presented in **Figures 2** and **3**. If the wavenumber is having low range, υ(C-C-O) band can be expected at 762 cm^{-1} and the CH wagging bands at 600 cm^{-1} by calculated method. It can be observed that the complex ring modes of CCC and CCN deformations occur in the range between 550 and 300 cm^{-1}. The methyl wagging band is demonstrated in the Raman spectrum at 257 cm^{-1} of weak region. The skeletal mode can be observed in the region between 50 to140 cm^{-1} in the Raman spectrum.

In general overall a good agreement was obtained between the experimental and theoretical frequency values as observed in **Table 3**. But even by using the quantum chemical calculations, it is complex to study for some of the molecular vibration assignments especially in the mid-low wavenumber range due to the mode mixing complexities. However major spectroscopic studies of the compound have been studied and assigned well in this study.

MEP analysis and Mulliken atomic charges

MEP is related to the electronic density and is a very useful descriptor in determining sites for electrophilic and nucleophilic reactions as well as hydrogen bonding interactions [14]. In addition, it displays the molecular shape, size and negative, positive and neutral electrostatic potential through color grading. The purpose of finding the electrostatic potential is to find the reactive site of a molecule. These maps allow us to visualize variably charged regions of a molecule. Knowledge of the charge distributions can be used to determine how molecules interact with 1 another. Total SCF electron density surface mapped with molecular electrostatic potential (MEP) of 4BAHEHMP are shown in **Figure 2**. The ascending order of electrostatic potential is red < orange < yellow < green < blue. According to the calculated results, the MEP map illustrates that the negative potential sites (electrophilic) are on oxygen and nitrogen atoms (N12) and the positive potential sites (nucleophilic) are around the hydrogen atoms. From these results we can say that the hydrogen atoms indicate the strongest attraction and the oxygen atom indicates the strongest repulsion.

Mulliken atomic charges calculation has a remarkable role in quantum chemical calculation applications to molecular system because these atomic charges have a great influence on dipole moment, molecular polarizability, electronic structure and other properties of molecular systems [15]. Mulliken populations can be used to characterize the electronic charge distribution in a molecule and the bonding, antibonding, or nonbonding nature of the molecular orbitals for particular pairs of atoms. Mulliken charges, in general, exhibit basis set dependency, which is always very high. From the description of atomic charge the processes of electro -negativity equalization and charge transfer in chemical reactions [16,17] can be obtained.

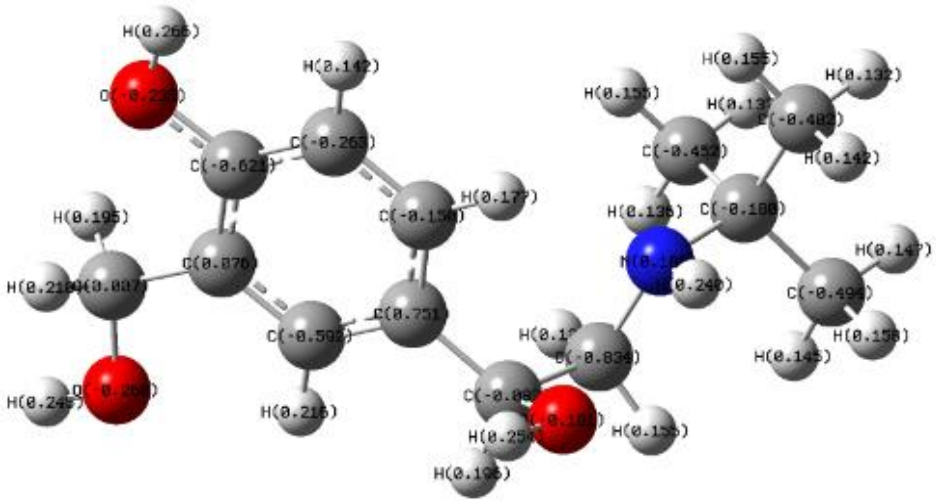

Figure 4 Mulliken atomic charges for 4BAHEHMP.

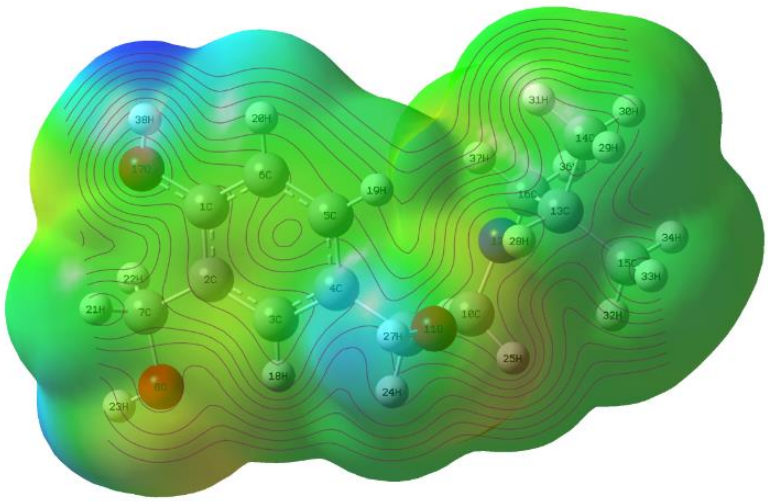

Figure 5 Molecular electrostatic potential (MEP) map for 4BAHEHMP.

Table 4 Mulliken atomic charges calculated by B3LYP/6-31++G (d,p) method.

Atom No.	B3LYP/6-31++G(d,p)	Atom No.	B3LYP/6-31++G(d,p)
C1	−1.079	H20	0.1276
C2	0.3976	H21	0.1936
C3	−0.6434	H22	0.1993
C4	0.5987	H23	0.2521
C5	0.1169	H24	0.2586
C6	−0.1544	H25	0.1144
C7	0.01622	H26	0.1609
O8	−0.2687	H27	0.2257
C9	−0.0618	H28	0.2294
C10	−0.7438	H29	0.1346

Atom No.	B3LYP/6-31++G(d,p)	Atom No.	B3LYP/6-31++G(d,p)
O11	−0.1393	H30	0.1416
N12	0.0898	H31	0.1534
C13	−0.3735	H32	0.1611
C14	−0.3568	H33	0.1525
C15	−0.5029	H34	0.1536
C16	−0.4426	H35	0.14
O17	−0.2186	H36	0.1522
H18	0.1977	H37	0.1548
H19	0.1917	H38	0.2702

In our methodology the calculation for Mulliken atomic charges have been performed using B3LYP/6-31++G(d,p) method. The atomic charges for the studied compound are picturized in **Figure 4** and were tabulated in **Table 4**. As indicated in **Table 4**, it is to be mentioned that some of the carbon atoms such as C2, C4, C5, C7 and nitrogen atom N12 of the title compound exhibit electropositivity while oxygen atoms O11 and O17 atoms exhibit negative charges. Carbon atom has a maximum negativity of about −1.079 in the C-OH group. The maximum positive atomic charge is represented for C4, the carbon present in the C-C functional group. However all the hydrogen atoms exhibit a net positive charge in 6-311++G(d,p) basis set. Since they are joined to electronegative atoms O, methyl and methylene groups in the diagram, the carbon atoms C1, C3, C6, C9, C10, C13, C14, C15 and C16 have negative values. The large area of electronegativity around oxygen atoms and net positivity on hydrogen and nitrogen atoms gives an idea of the formation of intermolecular interaction in solid forms [18,19].

Local reactivity descriptors

Fukui function plays an important role in examining the reactive sites like nucleophilic, electrophilic and radial attack of the molecule. These reactivity indexes are responsible for the selectivity of the molecule from the specific chemical events. In a molecule the more reactive regions are defined by the Fukui function of the system. From the observation of Mulliken atomic charges, neutral, cation and anion state of 4-[2-(tert-butylamino)-1-hydroxyethyl]-2-hydroxymethyl) phenol, Fukui functions (f_k^+;f_k^-; f_k^0) and local softness (sk+;sk-;sk^0) are calculated [20,21]. For a system of N electrons the total electrons present in anion, cation, and neutral states of molecules are given by N+1, N1 and N, respectively which are found from the independent computations. The gross charges qk(N+1), qk(N–1), and qk(N) are produced by Mulliken population analysis. The condensed Fukui functions are calculated by considering the following equations.

$f_k^+ = q_k(N + 1) – q_k(N)$ for nucleophilic attack

$f_k^- = q_k(N) – q_k(N - 1)$ for electrophilic attack

$f_k^0 = \frac{1}{2}[q_k(N + 1) – q_k(N - 1)]$ for radical attack

$S_k^+ = sf_k^+$; $S_k^- = sf_k^-$; $S_k^0 = sf_k^0$

where +, -, 0 signs represents the nucleophilic, electrophilic and radical attack, respectively.

Fukui functions and local softness for selected atomic sites 4-[2-(tert-butylamino)-1-hydroxyethyl]-2-(hydroxymethyl)phenol have been displayed in **Table 5**. The maximum values of all the 2 local electrophilic reactivity descriptors (f_k^+,S_k^+) at atom N12 indicate that this site is prone to nucleophilic attack. In the same way, the maximum values of the nucleophilic reactivity descriptors (f_k^-, S_k^-) at O17 indicate that this site can be more prone to electrophilic attack.

Table 5 Condensed fukui functions fk and descriptors (sf)k for 4BAHEHMP.

Atoms	fk+	fk−	fk0	(sf)k+	(sf)k−	(sf)k0
C1	−0.0438	0.1525	0.0544	−0.0075	0.0263	0.0094
C2	0.1087	−0.0478	0.0305	0.0187	−0.0082	0.0052
C3	0.0783	−0.0844	0.0031	0.0135	−0.0145	−0.0005
C4	0.1715	−0.0314	0.0701	0.0296	−0.0054	0.0121
C5	0.1332	−0.1016	0.0158	0.023	−0.0175	0.0027
C6	0.1741	−0.137	0.0186	0.03	−0.0236	0.0032
C7	0.0033	−0.0156	0.0062	0.0006	−0.0027	−0.0011
C8	0.3892	−0.3675	0.0109	0.0671	−0.0633	0.0019
C9	−0.0627	0.0535	0.0046	−0.0108	0.0092	−0.0008
C10	0.0915	−0.099	0.0038	0.0158	−0.0171	−0.0006
O11	0.3833	−0.3624	0.0105	0.0661	−0.0625	0.0018
N12	0.6188	−0.3608	0.129	0.1066	−0.0622	0.0222
C13	−0.0573	0.0566	0.0004	−0.0099	0.0098	−0.0001
C14	0.2827	−0.2887	−0.003	0.0487	−0.0498	−0.0005
C15	0.3204	−0.2992	0.0106	0.0552	−0.0516	0.0018
C16	0.291	−0.2915	0.0003	0.0502	−0.005	0
O17	0.4368	-0.3373	0.0498	0.0753	−0.0581	0.0086
H18	−0.1003	0.1162	0.008	−0.0173	0.02	0.0019
H19	−0.1037	0.109	0.0027	−0.0179	0.0188	0.0005
H20	−0.0837	0.0922	0.0043	−0.0144	0.0159	0.0007
H21	−0.0687	0.0878	0.0096	−0.0118	0.0151	0.0016
H22	−0.0626	0.0859	0.0117	−0.0108	0.0148	0.002
H23	0.2219	0.2287	0.0034	−0.0382	394	0.0006
H24	−0.0812	0.0988	0.0088	−0.014	0.017	0.0015
H25	−0.0228	0.0862	0.0317	−0.0039	0.0149	0.0055
H26	−0.0869	0.1001	0.0066	−0.015	0.073	0.0011
H27	−0.2333	0.2292	0.0021	−0.0402	0.0395	−0.0004
H28	−0.171	0.1827	0.0058	−0.0295	0.0315	0.001
H29	−0.0936	0.0998	0.0031	−0.0161	0.0172	0.0005
H30	−0.0903	0.1021	0.0059	−0.0156	0.0176	0.001
H31	−0.1011	0.1024	0.0007	−0.0174	0.0176	0.0001
H32	−0.0983	0.1023	0.002	−0.0169	0.0176	0.0003
H33	−0.0956	0.1015	0.003	−0.0165	0.0175	0.0005
H34	−0.0864	0.1023	0.008	−0.0169	0.0176	0.0014
H35	−0.0981	0.1006	0.0013	−0.0154	0.0173	0.0002
H36	−0.0892	0.105	0.0067	−0.018	0.0177	0.0011
H37	−0.1042	0.1023	0.0009	−0.0391	0.0176	−0.0002
H38	−0.2267	0.2293	0.0013	−0.0324	0.0395	0.0002

Thermodynamic properties

Some thermodynamic properties such as partition functions, enthalpy, internal energy, entropy, heat capacity and thermal energy have been found to be analytical in understanding of reactivity or mode of action. Using perl script Thermo.pl software [22], the thermodynamical parameters such as heat capacity, entropy and enthalpy have been calculated between the range of 100 K and 1,000 K for 4BAHEHMP and are listed in **Table 6**. From **Table 6**, it can be proved that all the thermodynamic values increases with the increase of temperature from 100 to1,000 K, which is related to the enhancement of the molecular vibration due to increase in temperature. The molecule's enthalpy H_m and entropy S_m variations suggests that it is more adjustable to change its thermodynamic system for temperature. The correlations between these thermodynamic properties and temperatures are fitted by quadratic formulas and corresponding fitting factors (R^2) for these thermodynamic properties are found to be 0.9993, 1 and 0.9994 for heat capacity, entropy, and enthalpy, respectively. The temperature dependence correlation graphs are shown in **Figure 5**. Scale factors have been recommended [23] for an accurate prediction in determining the heat capacities, entropies, and enthalpies.

Entropy $S^o_m = 252 + 09252\ T - 2\ X\ 10^{-4}\ T^2$; $R^2=1$
Specific Heat Capacity $C^o_{p,m}= 3.0088 + 0.9168\ T - 4\ X\ 10^{-4}\ T^2$; $R^2=0.9993$
Enthalpy $H^o_m = -9.7978 + 0.0995\ T+2\ X\ 10^{-4}\ T^2$; $R^2=0.9994$

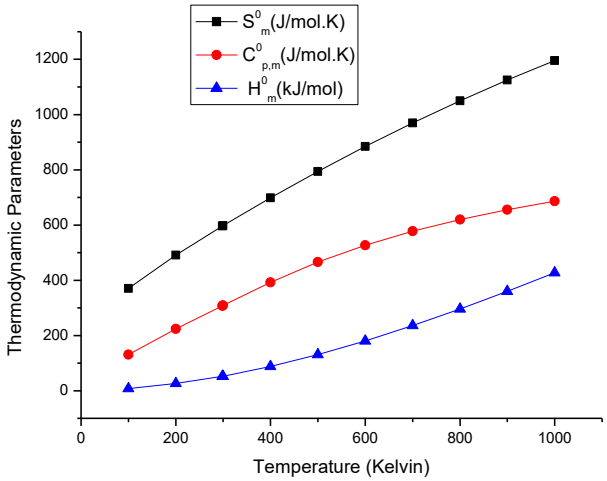

Figure 5 Correlation graphs of thermodynamic properties at different temperatures for 4BAHEHMP.

Table 6 Thermodynamic parameters at different temperatures at B3LYP/6-31++G(d,p) level for 4BAHEHMP.

T (K)	Entropy [J/mol.K]	Specific heat capacity [J/mol.K]	Enthalpy [kJ/mol]
100	370.83	130.89	8.06
200	491.12	223.49	25.95
298.15	596	307.64	52
300	597.91	309.23	52.57
400	698.46	392.66	87.73
500	794.19	466	130.76
600	884.73	527.11	180.51
700	969.9	577.67	235.83
800	1,049.88	619.96	295.77
900	1,125.02	655.79	359.61
1,000	1,195.74	686.45	426.76

It is observed that the thermodynamic parameters provide unique information regarding the further investigation on the title compound. The thermodynamical parameters were observed to be in proportional to the temperature due to equipartition energy. They are used to compute the thermodynamic energies from the relationship between thermodynamic functions and the estimation of the directions of chemical behavior by the second law of thermodynamics in the thermo-chemical field [24].

Conclusions

Geometry of 4-[2-(tert-butylamino)-1-hydroxyethyl]-2-(hydroxymethyl)phenol was optimized and investigated using DFT at B3LYP level of theory employing 6-31++G(d,p) basis set. Spectroscopic characterization such as FT-IR and FT-Raman were performed. The experimental and scaled vibrational wavenumbers have a high degree of correlation, allowing for simple assigning of various vibrational modes. From the Mulliken atomic charge studies it can be seen that the large area of electronegativity around O atoms and net positivity on H and N atoms gives an idea of the formation of intermolecular interaction in solid forms. From the Fukui function studies it can be concluded that the maximum values of the two local electrophilic reactivity descriptors at atom N12 suggests that this site is prone to nucleophilic attack. Similarly, the maximum values of the nucleophilic reactivity descriptors at O17 suggests that this site is more prone to electrophilic attack. Correlations between statistical thermodynamic data and temperature have been found. The chemical and thermal stability of the compound was computed by using DFT method for various temperatures and it shows that thermodynamic parameters increase with increase in temperature. In conclusion, the studies presented in the present research would be helpful for the researchers dealing with computational chemistry.

Acknowledgements

The author would like to acknowledge SAIF IIT Chennai for FTIR and FT-Raman measurements.

References

[1] HR Ali, HG Edwards, J Kendrick and IJ Scowen. Vibrational spectroscopic study of salbutamol hemisulphate. *Drug Test. Anal.* 2009; **1**, 51.
[2] L Rhyman, P Ramasami, JA Joule, JA Sáez and LR Domingo. Understanding the formation of [3+2] and [2+4] cycloadducts in the lewis acid catalysed reaction between methyl glyoxylate oxime and cyclopentadiene: A theoretical study. *RSC Adv.* 2013; **3**, 447.
[3] E Barim and F Akman.Synthesis, characterization and spectroscopic investigation of N-(2-acetylbenzofuran-3-yl)acrylamidemonomer: Molecular structure, HOMO–LUMO study, TD-DFT and MEP analysis. *J. Mol.Struct.* 2019; **1195**, 506-13.
[4] MJ Frisch GW Trucks, HB Schlegel, GE Scuseria, MA Robb and JR Cheeseman. *Gaussian 03 revision E.01*. Gaussian, Wallingford CT, 2004.
[5] C Lee, W Yang and RG Parr. Development of the colle-salvetti correlation-energy formula into a functional of the electron density. *Phys. Rev. B* 1988; **37**, 785.
[6] M Uzzaman and MN Uddin. Optimization of structures, biochemical properties of ketorolac and its degradation products based on computational studies. *DARU J. Pharmaceut. Sci.* 2019; **27**, 71-82.
[7] AD Becke. Density-functional thermochemistry. III. the role of exact exchange. *J. Chem. Phys*. 1993; **98**, 5648.
[8] A Frisch, AB Nielson and AJ Holder. *GUASSVIEW user manual*. Guassian, Connecticut, 2000.
[9] JA Bis, PD Boyle, SAR Carino, DH Igo and LM Katrincic. Crystallization and Solid-State Characterization of the Hemihydrate of Albuterol Hemisulfate. *Cryst. Growth Des.* 2014; **14**, 775.
[10] JM Leger, M Goursolle and M Gadret. Structure cristalline du sulfate de salbutamol [tert-butylamino-2(hydroxy-4 hydroxyméthyl-3 phényl)-1éthanol.0.5H2SO4]. *Acta Crystallogr. B* 1978; **34**, 1203.
[11] AP Scott and L Radom.Harmonic vibrational frequencies: An evaluation of hartree-fock, møller-plesset, quadratic configuration interaction, density functional theory, and semiempirical scale factors. *J. Phys. Chem.* 1996; **100**, 16502-13.
[12] T Kuppens, K Vandyck, JVD Eycken, W Herrebout, BVD Veken and P Bultinck. A DFT conformational analysis and VCD study on methyl tetrahydrofuran-2-carboxylate. *Spectrochim. Acta A Mol. Biomol. Spectros.* 2007; **67**, 402-11.
[13] DO Corrigan, OI Corrigan and AM Healy. Physicochemical and *in vitro* deposition properties of salbutamol sulphate/ipratropium bromide and salbutamol sulphate/excipient spray dried mixtures for use in dry powder inhalers. *Int. J. Pharm.* 2006; **322**, 22.

[14] S Sarala, SK Geetha, S Muthu and FB Asif. Vibrational spectra and wavefunction investigation for antidepressant drug of amoxapine based on quantum computational studies. *Chem. Data Collect.* 2021; **33**, 100699.
[15] T Subramanian, SA Bahadur, A Manikandan and S Athimoolam. Structural, spectroscopic investigation and computational study on nitrate and hydrogen oxalate salts of 2-aminopyrimidine. *J. Nanosci. Nanotechnol*. 2018; **18**, 2450-62.
[16] K Jug and ZB Maksic. *Theoretical model of chemical bonding, part 3.* Springer, Berlin, Germany, 1991.
[17] M Govindrajan, M Karabacak, A Savitha and S Periandy. FT-IR, FT-Raman, ab initio, HF and DFT studies, NBO, HOMO–LUMO and electronic structure calculations on 4-chloro-3-nitrotoulene. *Spectrochim. Acta Mol. Biomol. Spectros.* 2012; **89**, 137.
[18] RP Gangadharan and SS Krishnan. Experimental and computational study on molecular structure and vibrational analysis of hydroxybenzopyridine using DFT method. *Asian J. Chem.* 2014; **26**, 4571.
[19] HL Xiang, XR Liu and XZ Zhang. Calculation of vibrational spectroscopic and NMR parameters of 2-Dicyanovinyl-5-(4-N,N-dimethylaminophenyl) thiophene by ab initio HF and Density functional methods. *Comput. Theor. Chem.* 2011; **969**, 27.
[20] P Bultinck, R Carbo-Dorca and W Langenaeker. Negative fukui functions: New insights based on electronegativity equalization. *J. Chem. Phys.* 2003; **118**, 4349.
[21] RP Gangadharan and SS Krishnan. Quantum chemical calculations on 4-[2-(Tert-Butylamino)-1-Hydroxyethyl]-2-(Hydroxymethyl)phenol by density functional theory. *Spectros. Spectral Anal.* 2018; **38**, 3631-7.
[22] M Vimala, SS Mary, R Ramalakshmi and S Muthu. Theoretical description of green solvents effect on electronic property and reactivity of Tert-butyl 4-formylpiperidine-1-carboxylate. *Comput. Theor. Chem.* 2021; **1201**, 113255.
[23] A Nataraj, V Balachandran and T Karthick. Molecular orbital studies (hardness, chemical potential, electrophilicity, and first electron excitation), vibrational investigation and theoretical NBO analysis of 2-hydroxy-5-bromobenzaldehyde by density functional method. *J. Mol. Struct*. 2013; **1031**, 221.
[24] R Zhang, B Dub, G Sun and Y Sun. Experimental and theoretical studies on o-, m- and p-chlorobenzylideneaminoantipyrines. *Spectrochim. Acta A Mol. Biomol. Spectrosc.* 2010; **75**, 1115-24.